PROCEEDINGS B

royalsocietypublishing.org/journal/rspb

Research

Cite this article: Huie JM, Park G, Kawano SM. 2025 Salamander ecomorphology reveals a unique suite of climbing adaptations. *Proc. R. Soc. B* **292**: 20251295.
https://doi.org/10.1098/rspb.2025.1295

Received: 18 May 2025
Accepted: 31 July 2025

Subject Category:
Morphology and biomechanics

Subject Areas:
biomechanics, evolution

Keywords:
allometry, *Aneides*, clinging, gripping, many-to-one mapping, Plethodontidae

Author for correspondence:
Jonathan M. Huie
e-mail: jonathanmhuie@gmail.com

Electronic supplementary material is available online at https://doi.org/10.6084/m9.figshare.c.7963826.

THE ROYAL SOCIETY
PUBLISHING

Salamander ecomorphology reveals a unique suite of climbing adaptations

Jonathan M. Huie[1], Grace Park[1] and Sandy M. Kawano[1,2]

[1]Biological Sciences, The George Washington University, Washington, DC 20052, USA
[2]Biology, University of Virginia, Charlottesville, VA 22903, USA

JMH, 0000-0002-7925-7372; SMK, 0000-0002-1856-5566

Many salamanders climb extensively but lack morphological adaptations, such as claws or adhesive toe pads, found in other climbing tetrapods. Here, we compared climbers and non-climbers from the salamander genera *Aneides* and *Plethodon* to evaluate potential morphological adaptations for climbing across multiple levels of biological organization. We integrated body shape morphometrics, allometry of the autopods (manus and pes), mechanical advantage of the digits and comparisons of epithelial microstructures. Compared with non-climbers, climbers have longer limbs that likely facilitate faster climbing and have larger and positively allometric autopods that likely yield superior clinging performance. Longer digits increase climbing reach at the expense of grip force, but climbers circumvent this trade-off with phalangeal morphologies that increase the mechanical advantage of their digits. A few species also have pes epithelia that may increase adhesion or friction but epithelial morphology was largely uncorrelated with habitat use. While scansorial species of *Aneides* and *Plethodon* share some characteristics with other genera of climbing salamanders, our results reveal subtle differences between rock-climbing and tree-climbing salamanders that reflect distinct selective pressures imposed by their microhabitats. Many-to-one mapping enables alternate strategies to address the challenges of climbing and helps to explain the abundance and diversity of climbing tetrapods.

1. Introduction

Many-to-one mapping explains how different suites of morphological traits can achieve the same performance [1]. Many factors can influence phenotypic variation and limit morphological convergence (e.g. trade-offs, developmental constraints and genetic variation); as a result, animals have evolved diverse strategies to overcome similar challenges [2–4]. For instance, the propensity to climb (scansoriality) exposes animals to more pronounced gravitational and shear forces compared with horizontal walking, which promotes traits that increase friction and adhesion [5–8]. Claws are common adaptations for gripping and have convergently evolved across invertebrates and vertebrates [5,9,10]. Many tree-climbing (arboreal) lizards also have adhesive toe pads that provide access to a wider range of habitats [9,11–13]. However, many climbing tetrapods do not have claws or toe pads [14,15]. Lungless salamanders (Plethodontidae), in particular, have undergone multiple transitions towards arboreality but lack obvious adhesive structures [15–17]. Plethodontids provide the opportunity to investigate climbing strategies in the absence of specialized morphologies.

Climbing salamanders (*Aneides* spp.) are the only temperate plethodontids that consistently utilize arboreal habitats [16] (figure 1). The genus includes species like *Aneides vagrans*, which is renowned for its ability to climb redwood trees up to 93 m above the ground [18,19]. Some *Aneides* species are more saxicolous, in that they often climb rock structures, but venture into trees during the summer [20,21]. A few morphological characteristics of *Aneides* have been purported as adaptations for climbing, such as long limbs and digits, squared toe tips and recurved terminal phalanges with large ventral processes [22–24]. However, it is not clear how these morphological traits improve climbing performance. Furthermore, there may be nuanced ecomorphological differences between arboreal and saxicolous *Aneides* species. Lizards often have limb morphologies that match the structural differences of their microhabitats (i.e. substrate width and texture) [11,13,25], but this pattern has not been investigated in *Aneides* salamanders.

Examination of the autopods (manus and pes) may yield insights into how some *Aneides* species are adapted for clinging, gripping and ultimately climbing. Salamanders use a layer of mucus covering their bodies to cling to surfaces [26,27]. Biomechanical models and empirical data suggest their clinging performance is predicted by autopod contact area but not autopod shape [17,27,28]. A few cave-dwelling salamanders (*Chriopterotrion magnipes* and *Speleomantes* spp.) grow disproportionately large pedes, possibly reflecting increased selection on pes size to improve clinging performance on cave walls [29,30]. Moreover, many arboreal and saxicolous frogs have evolved toe pads with hexagonal epithelial cells separated by deep channels and covered in peg-like nanostructures that disperse mucus across the skin, increasing wet adhesion and friction through more contact with surface asperities [31]. Salamanders may have similar epithelial morphologies on their autopods, which would increase the clinging effectiveness of their autopods [15,26,27].

Lastly, some salamanders augment their attachment to rough surfaces by mechanically gripping the surface with their digits [19,26]. While longer digits extend the reach of climbers, they generate lower gripping forces than shorter digits with an otherwise comparable morphology, presenting a functional trade-off between reach versus force [32]. However, larger ventral processes on the terminal phalanges affect the insertion of the digital flexors and may increase the mechanical advantage and gripping force of the digits in climbing species [22,24]. Scansorial species of *Aneides* may also exhibit greater dorsoventral curvature of the terminal phalanges to reduce bone strain while gripping [33].

We compared the functional morphology of climbing and non-climbing species of *Aneides* to assess whether the limbs of scansorial species may be adapted for scansoriality. We also examined three *Plethodon* species, which are closely related to *Aneides* and span a similar gradient between climbing versus ground-dwelling. Our objectives were to: (i) assess the relationship between body shape and habitat preference, (ii) contrast autopod allometry between climbers and non-climbers, (iii) quantify the mechanical advantage of the phalanges for gripping, and (iv) examine potential adaptations for adhesion or friction in the microstructure of pes epithelia. We predicted that climbing species exhibit longer limbs, positive autopod allometry, higher mechanical advantage in their digits and pes epithelia with deep intercellular channels and peg-like nanostructures compared with non-climbing species. We also predicted that these traits may differ between arboreal and saxicolous species. We found support for most of our hypotheses, indicating that a suite of subtle morphological changes likely improves climbing abilities in *Aneides*. Our findings further demonstrate that claws and adhesive toe pads are beneficial for climbing but not required; climbing can evolve in other tetrapods through alternate strategies involving only subtle changes to their morphology.

2. Methods

(a) Habitat categorization and reconstruction

We generated morphological data for all 10 species of *Aneides* and three species of *Plethodon* (*P. elongatus*, *P. glutinosus* and *P. petraeus*). Based on the literature, each species was categorized as a climber or non-climber and then subdivided based on its primary habitat preferences (electronic supplementary material, table S1). Half of the *Aneides* are scansorial (arboreal or saxicolous), while the remaining species are ground-dwellers (terrestrial). *Plethodon petraeus* is saxicolous, whereas *P. glutinosus* is primarily terrestrial but facultatively climbs on rocks and logs. These *Plethodon* species co-exist with *A. aeneus* and occur syntopically at some localities [34,35]. Meanwhile, *P. elongatus* is fully terrestrial and overlaps in distribution with some *Aneides* species in the western United States.

To investigate the origin of scansoriality in *Aneides*, we reconstructed the evolutionary history of habitat use with a recent time-calibrated salamander phylogeny [36]. We pruned the tree to include 30 plethodontid species, including our focal taxa and 17 additional species that we later used to investigate the evolutionary allometry of pes size across plethodontids more broadly (see below). Then, we performed a stochastic character mapping with 1000 simulations using the 'make.simmap' function in the *phytools* R package v. 2.4 [37]. The analysis was conducted with an equal-rates transition model, which was determined to be a better fit than a symmetrical rates model and all-rates-different based on Akaike Information Criterion (AIC) scores. All analyses in this study were performed in R v. 4.3.2 [38].

(b) Body shape measurements

We examined 411 preserved specimens of *Aneides* and *Plethodon,* with an average of 32 ± 8 s.d. (range: 15–47) specimens per species that spanned the size range of each species (electronic supplementary material). Each specimen was photographed in the dorsal and ventral views with its digits splayed out using a Nikon D800E Digital SLR equipped with a 105 mm macro lens, an iPhone 11 or an iPhone 13. We prioritized specimens with minimal distortion, all of their limbs and a complete tail. However, we also used individuals of *A. caryaensis* and *P. elongatus* with partial tails due to the limited availability of specimens. We sampled males and females instead of a single sex because our preliminary analyses indicated that *Aneides* exhibit minimal sexual dimorphism in their limbs (electronic supplementary material).

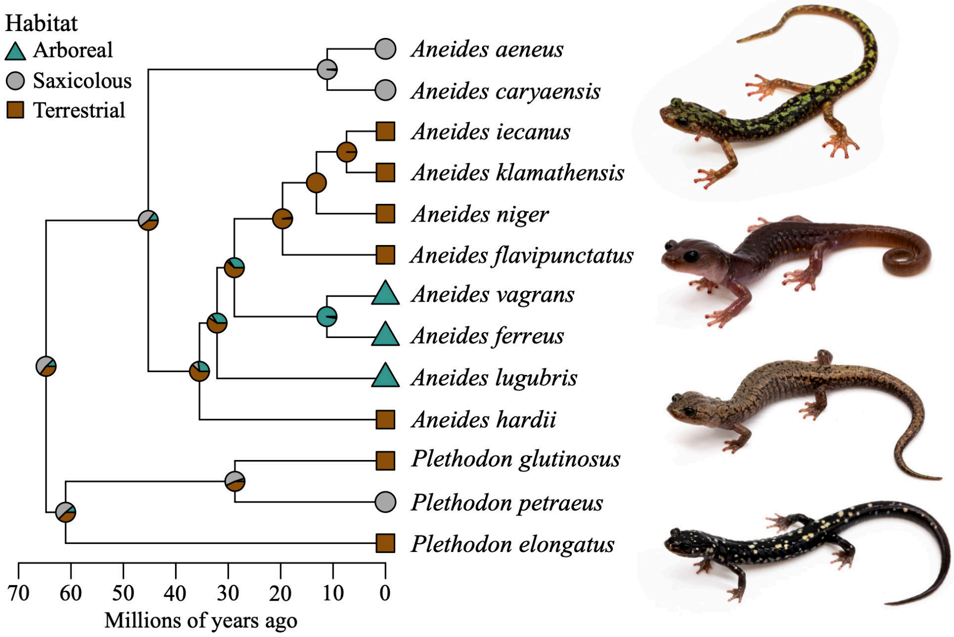

Figure 1. Phylogenetic relationships of the focal species of *Aneides* and *Plethodon*. Tip shapes depict microhabitat preferences, while pies at the internal nodes depict likelihood values from an ancestral state reconstruction. Photos of representative species from top to bottom: *A. aeneus, A. hardii, A. lugubris* and *P. glutinosus* (not to scale).

To compare body shape between climbers and non-climbers, we quantified eight morphological traits often related to locomotion and habitat use [39,40]. These included: snout-vent length (SVL), tail length, forelimb length, hindlimb length, length of the longest (third) digit on the manus, length of the longest (third) digit on the pes, surface area of the manus and surface area of the pes (figure 2*a*). Most measurements were taken from photographs using FIJI v. 2.3 [41]. The autopod area was measured by tracing its perimeter and calculating the enclosed area in FIJI. In this study, autopod referred to the distal regions of the limbs that included the manus (carpals, metacarpals and phalanges) in the forelimbs or the pes (tarsals, metatarsals and phalanges) in the hindlimbs. Because the limbs were often fixed in variable poses, we used digital callipers to measure the limb segments (e.g. upper arm/leg and lower arm/leg) to the nearest 0.1 mm and then summed the segments to calculate limb length. We also weighed each individual to the nearest 0.01 g and then subtracted the weight of their specimen tag. For specimens with partial tails, we regressed the tail length and body mass of complete specimens against SVL on a log–log scale and used the resulting species-specific equations to estimate the missing tail and mass data.

To visualize intraspecific and interspecific variation in body shape, we performed a principal component analysis (PCA). We first log-transformed the limb and tail measurements, regressed them against log(SVL) and used the residuals from the regressions as size-corrected variables. We performed the PCA with a covariance matrix on the residuals using the 'prcomp' function in the *stats* R package v. 4.4.1 [38]. We plotted intraspecific variation and mean values for each species with the phylogeny overlaid to show the phylogenetic relationships.

(c) Allometry of autopod size

We investigated the static allometry of the manus and pes area (A) relative to body mass (W) for each species, assuming the allometric equation

$$A = bW^{\alpha},$$

where α represents the relative growth parameter and b represents the relative autopod area. On a log–log scale, the allometric relationship is linear: $\log(A) = \log(W) \times \alpha + \log(b)$, where α is the static allometric slope and $\log(b)$ is the static allometric intercept. We hereafter refer to α and b as the slope and intercept, respectively. We estimated these coefficients using ordinary least squares regressions with the *smatr* R package v. 3.4 [42]. Scaling relationships were considered positively allometric if the 95% confidence interval (CI) of the calculated slopes was above the expected isometric relationship between area and mass (slope = 0.66). We used the non-phylogenetic 'procD.lm' function in the *geomorph* R package v. 4.0.8 [43] to compare the average static slope and autopod size between habitat groups.

We compared the scaling coefficients for *Aneides* and *Plethodon* with published values for the pes of 17 additional plethodontid species (*Chiropterotriton magnipes*, 10 *Bolitoglossa* and 6 *Speleomantes*) [29,30] (electronic supplementary material, table S1). We re-analysed the *Speleomantes* data from [30] to extend their reported coefficients at the genus level to species-specific coefficients. The maximum SVL, locomotor mode (climbing versus non-climbing) and habitat preferences were assessed for each species (electronic supplementary material, tables S1 and S8). We used the SVLs to estimate the maximum body mass of all 30 species using a length–mass equation for plethodontid salamanders [44]. Then we estimated the maximum pes area of each species using the species-specific scaling coefficients. We used the 'procD.pgls' function in *geomorph* to perform phylogenetic

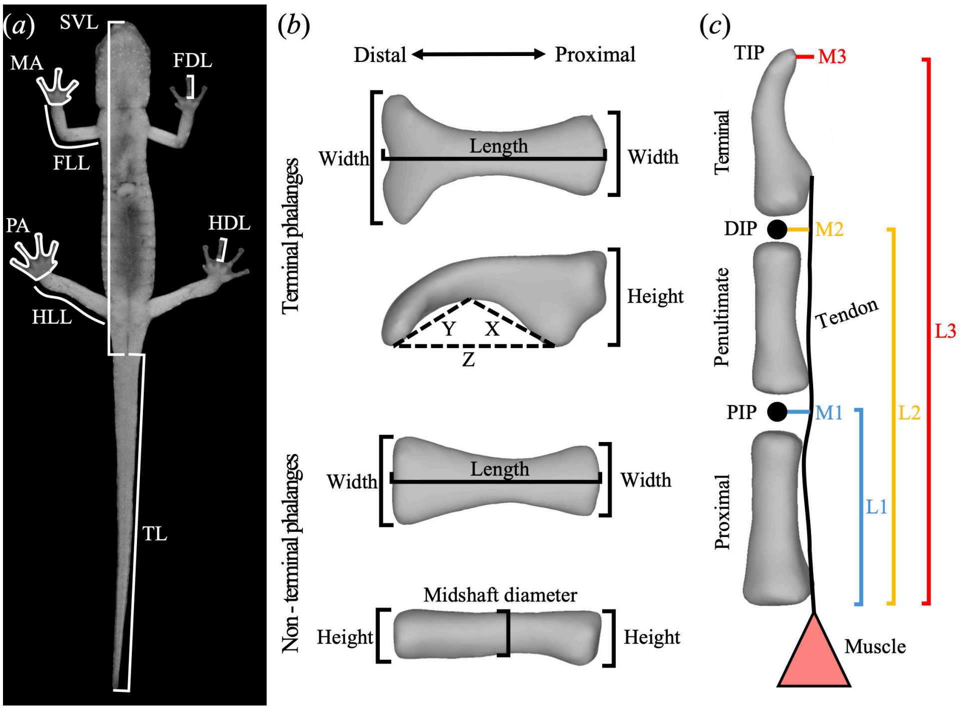

Figure 2. Diagram of the morphological measurements. (*a*) Body shape measurements: SVL, tail length (TL), forelimb length (FLL), longest finger length (FDL), manus area (MA), hindlimb length (HLL), longest toe length (HDL) and pes area (PA). (*b*) Measurements of X, Y and Z were used to measure curvature in the phalanges, depicted in dorsal and lateral views. (*c*) Anatomical model based on [32]; used to measure mechanical advantage at the proximal interphalangeal (PIP) joint, distal interphalangeal (DIP) joint and at the tip (TIP) as the ratios between the lengths of the moment arm (M1–3) and load arm (L1–3).

least squares regressions to compare the evolutionary allometric slopes and relative pes size between habitat groups, while accounting for phylogenetic non-independence. While static allometry refers to pes size relative to body mass within a species, evolutionary allometry refers to the relationship across species.

(d) Functional morphology of the phalanges

To investigate the gripping potential of climbers and non-climbers, we compared the phalanges of our 13 focal taxa with micro-computed tomography (μCT) scans. We acquired one μCT scan per species from MorphoSource.org [45,46] or by obtaining new scans (electronic supplementary material, table S2). New scans were generated using a General Electric Phoenix v|tome|x m 240 at the Smithsonian National Museum of Natural History Imaging Facility, with a voxel size between 27 and 45 μm, 80 kV, 230–240 μA and an exposure time between 250 and 333 ms.

We selected one of the longest fingers and toes from each specimen, favouring digits that were straighter and undamaged. We segmented and measured the three phalanges of each digit in three-dimensional (3D) Slicer v. 5.6.2 [47,48]. From the ossified portions of the proximal and penultimate phalanges, we took six measurements following published methodologies [32]. These traits included phalangeal length, midshaft diameter, proximal end height, proximal end width, distal end height and distal end width (figure 2*b*). We also took five measurements from the terminal phalanx that included phalangeal length, proximal end height, proximal end width, distal end width and curvature (figure 2*b*). Using the equation commonly used to calculate claw curvature [49], we calculated phalangeal curvature as:

$$\text{curvature} = 57.296 \times (2\sin^{-1}(2X^2Y^2 + 2Y^2Z^2 + 2X^2Z^2 - X^4 - Y^4 - Z^4)^{0.5}/2XY),$$

where X is the distance from the ventral base of the phalanx to the vertex of the ventral curve, Y is the distance from the ventral vertex to the tip of the phalanx and Z is the distance from the ventral base of the phalanx to the tip of the phalanx. Measurements of X, Y, Z and the terminal phalanx length were collected from lateral photos of the phalanx in FIJI. All linear measurements were divided by digit length to reduce the effects of size. We analysed variation in the size-independent phalangeal measurements (ratios and curvature) from the manus and pes with a PCA using the ‘prcomp’ R function, performed with a correlation matrix to account for the different units of these measurements.

We measured mechanical advantage as a proxy for gripping force, assuming a neutral and straightened position. We accounted for postural variation by straightening the digits using the ‘Curved Planar Reformat’ module in 3D Slicer. This method maintains spacing between the phalanges but causes minimal distortion to the shape of the phalanges. Thus, we used the ‘FastModelAlign’ module [48] to map the original phalanges onto the position of the distorted bones. Minor adjustments to phalangeal position and orientation were made using the ‘Transforms’ module. To measure mechanical advantage, we assumed a simple anatomical model with a single flexor tendon that inserts on the ventral process of the terminal phalanx (figure 2*c*) [32]. We measured the tendon moment arms at each joint and allowed the load arm to increase along a proximodistal gradient [32].

Mechanical advantage at the proximal interphalangeal (PIP) joint, distal interphalangeal (DIP) joint and the tip of the digit (TIP) were then calculated by taking the ratio between the moment arm and load arm.

(e) Relationship between habitat and morphology

We tested for associations between morphology and habitat with one-way ANOVAs. A separate phylogenetic ANOVA was performed for each size-independent body shape trait (averaged by species), size-independent phalangeal measurement, mechanical advantage at each joint and total mechanical advantage summed across the joints. These analyses were performed using the 'procD.pgls' function in *geomorph*. For significant tests (alpha level = 0.05), pairwise comparisons between habitat groups were conducted with a Holm–Bonferroni correction to reduce the probability of type I errors associated with conducting multiple statistical tests.

(f) Scanning electron microscopy of the pes

To investigate whether climbing species have epithelial morphologies on their pedes that aid in adhesion, we examined the ventral surface of the pes in nine focal species using scanning electron microscopy. We dissected pedes from specimens in natural history collections or the authors' personal collection (electronic supplementary material, table S3). All specimens were fixed in 10% neutral-buffered formalin and stored in 70% ethanol. The authors' specimens were frozen for less than a month and thawed before fixation, but appeared undamaged. Samples were dehydrated with an ethanol series and moved into 100% ethanol 24 h prior to being critical point dried (Tousimis Autosamdri 815) and sputter coated with gold palladium (Denton Vacuum Desk V). Whole pedes were imaged using a Zeiss Evo 10 scanning electron microscope (Carl Zeiss AG). We also estimated the density of potential mucus pores on the soles and toes using micrographs with magnifications between 300× and 450× (electronic supplementary material, figure S1).

3. Results

(a) Habitat evolution in *Aneides*

Our evolutionary reconstruction of habitat use indicated that the ancestor of *Aneides* was most likely scansorial. Specifically, it had the highest likelihood of being saxicolous (46%), compared with being arboreal (15%) or terrestrial (39%; figure 1 and electronic supplementary material, figure S2). The reconstruction also indicated that arboreality may have independently evolved from terrestriality twice, once in the ancestor of *A. lugubris* and a second time in the ancestor of *A. ferreus*+*A. vagrans*.

(b) Ecomorphological variation in body shape

Arboreal, saxicolous and terrestrial salamanders occupied unique regions of morphospace (figure 3). The first principal component (PC1; 80.5% of the variation) described variation in limb length, digit length and autopod area; while PC2 (10.6% of the variation) reflected variation in tail length (electronic supplementary material, table S4). Arboreal and saxicolous species had longer limbs, longer digits and larger autopods than terrestrial species, but saxicolous species had slightly longer limbs and larger extremities than arboreal species. The sampled *Plethodon* species had longer tails than most *Aneides,* regardless of their habitat preferences. The saxicolous *P. petraeus* had forelimb morphologies that were, on average, not as long nor as large as those in the saxicolous *Aneides* but still longer than those of terrestrial *Plethodon* species. *Plethodon glutinosus* had longer limbs than the terrestrial *Aneides*, while *P. elongatus* had the shortest limbs of all the species examined in our study.

Phylogenetic ANOVAs supported these results and revealed significant variation related to habitat use in all traits ($p \le 0.050$; electronic supplementary material, table S5). Saxicolous species had significantly longer tails than arboreal species ($p = 0.038$), but no other pairwise comparison was significant between the two groups ($p \ge 0.522$). In contrast, all comparisons between saxicolous species and terrestrial species were significant ($p \le 0.039$). Arboreal species only had significantly longer fingers ($p = 0.024$) and toes ($p = 0.048$) than terrestrial species.

(c) Allometry of autopod size

The autopods of all *P. petraeus* and all *Aneides* species scaled with positive static allometry relative to body mass, while those of *P. elongatus* and *P. glutinosus* scaled with isometry (electronic supplementary material, table S6). Habitat had a significant effect on the static slope of the manus ($F_2 = 2.767$, $p = 0.048$) but not the pes ($F_2 = 1.151$, $p = 0.306$). Saxicolous species exhibited a shallower pes slope (slope = 0.73) than arboreal species (slope = 0.79; $Z = 1.92$, $p = 0.016$; figure 4*a*), while all other pairwise comparisons were non-significant ($p \ge 0.134$; electronic supplementary material, table S7). Habitat had a significant effect on the relative size of the manus ($F_2 = 208.34$, $p = 0.001$) and pes ($F_2 = 247.72$, $p = 0.001$), with all pairwise comparisons being significant ($p \le 0.001$; electronic supplementary material, table S7). Saxicolous species had proportionally the largest autopods, followed by arboreal species and then terrestrial species (figure 4*a,b*). Overall, there was considerable variation in the static allometric slope

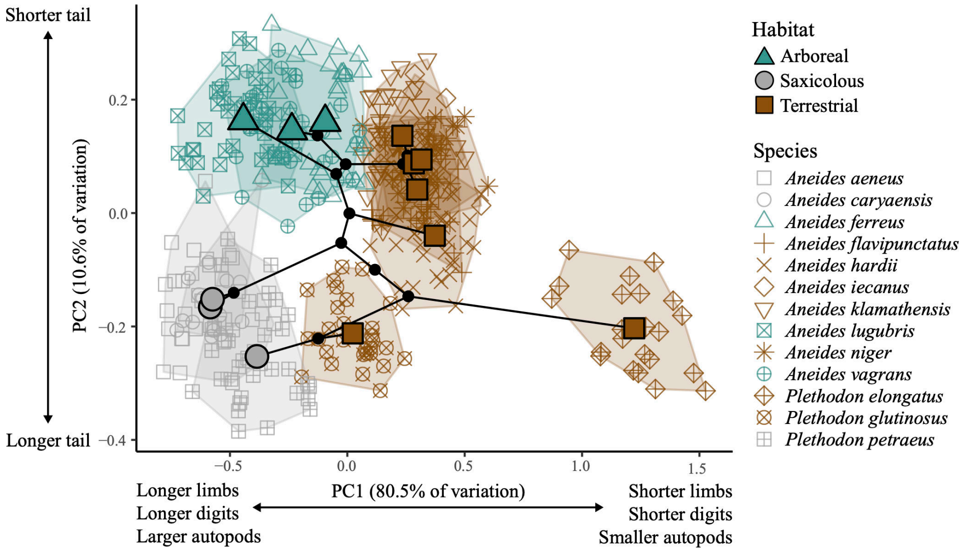

Figure 3. Phylomorphospace showing variation in body shape. Each small, unfilled symbol represents an individual, while the convex hulls depict intraspecific variation. Larger filled symbols represent species means (n = 15–47 individuals per species). The black branching lines depict the phylogenetic relationships between species.

and intercept of the pes across 30 species of plethodontid salamanders (slope = 0.66–0.946; intercept = 0.06–0.21; figure 4*c* and electronic supplementary material, table S8).

The common evolutionary allometric slope across all 30 species was 0.64 (95% CI = 0.55–0.72), indicating that salamander species exhibit evolutionary isometry (figure 4*d*). Habitat did not have a significant effect on the evolutionary allometric slope ($F_2 = 0.825$, $p = 0.441$; electronic supplementary material, table S9). However, habitat did have a significant effect on relative pes size ($F_2 = 20.192$, $p = 0.001$). Saxicolous species had significantly larger pes than arboreal ($Z = 1.852$, $p = 0.021$) and terrestrial species ($Z = 3.30$, $p = 0.001$; electronic supplementary material, table S9). Arboreal species also had larger pes sizes than terrestrial species ($Z = 1.797$, $p = 0.033$; figure 4*d*).

(d) Functional variation of phalangeal morphology

Phalanges of the fingers and toes were characterized by similar axes of variation that distinguished scansorial species from terrestrial species (figure 5*a*). Along PC1 (70.5% of the variation) and PC2 (10.6% of the variation), arboreal and saxicolous species occupied overlapping regions of the phalangeal morphospace (electronic supplementary material, table S10). Scansorial species differed from terrestrial species by having smaller proximal phalanges (in all anatomical directions), narrower and shorter penultimate phalanges, and slightly longer penultimate and terminal phalanges (figure 5*a*). The terminal phalanges of arboreal and saxicolous species were more recurved, laterally expanded at the tip and had a larger ventral process (figure 5*a*). In contrast, the terminal phalanges of *P. elongatus* were dorsoventrally flatter and more pointed at the tip. Most of the terrestrial species were intermediate to the scansorial species and *P. elongatus*, in that the former exhibited some curvature and lateral expansion at the tip. The phalangeal morphology of *P. petraeus* was most similar to members of the *A. flavipunctatus* complex but notably different from other *Plethodon* species.

However, the phylogenetic ANOVAs did not indicate a strong association between habitat and phalangeal morphology (electronic supplementary material, tables S11 and S12). Significant variation in the finger phalanges associated with habitat ($p \leq 0.049$) was found in the width and height of the proximal and penultimate phalanges, as well as the size of the ventral process on the terminal phalanges (electronic supplementary material, table S11). The toes exhibited similar patterns in the proximal and penultimate phalanges as well as significant variation in the curvature of the terminal phalanges ($p \leq 0.029$; electronic supplementary material, table S12).

Mechanical advantage also differed between habitat groups (electronic supplementary material, tables S11 and S12; figure 5*b*,*c*). At the PIP joints for both the fingers and toes, terrestrial species had the highest mechanical advantage, but there was substantial overlap between groups. At the DIP joints, saxicolous species had significantly higher mechanical advantage than terrestrial species ($p \leq 0.042$), while arboreal species were intermediate between them. Similar patterns were observed at the tips of the digits, but only the toes of saxicolous species differed significantly from terrestrial species ($Z = 1.96$, $p = 0.036$). When mechanical advantage was summed across the joints, values for saxicolous species were significantly 1.2–1.3× higher than those for arboreal and terrestrial species (electronic supplementary material, table S12).

(e) Surface epithelium of the pes

Species examined herein had smooth surfaces on the ventral side of the pes and toe pads on the macroscale but variable skin morphology at the micro- and nanoscale (figure 6). The epithelia consisted of irregular polygonal cells in all species (figure 6). Most species lacked distinct intercellular channels, except for *A. aeneus* and *A. hardii* (figure 6*a*–*g*). Both species had channels

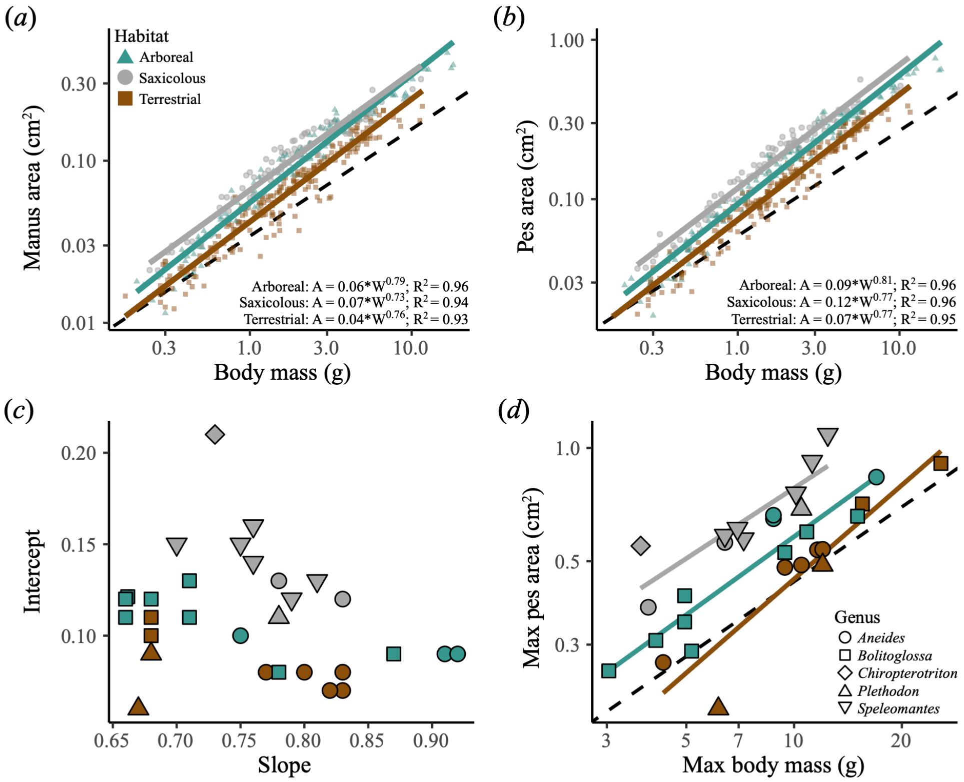

Figure 4. Allometry of autopod size (*A*) relative to body mass (*W*). Static allometry of the (*a*) manus and (*b*) pes for species in *Aneides* and *Plethodon*, grouped by habitat. (*c*) Variation in static scaling coefficients for 30 species of plethodontid salamanders. (*d*) Evolutionary allometry of estimated pes area and maximum body mass across five genera of salamanders. In all panels, the black dotted line represents the isometric slope (0.66).

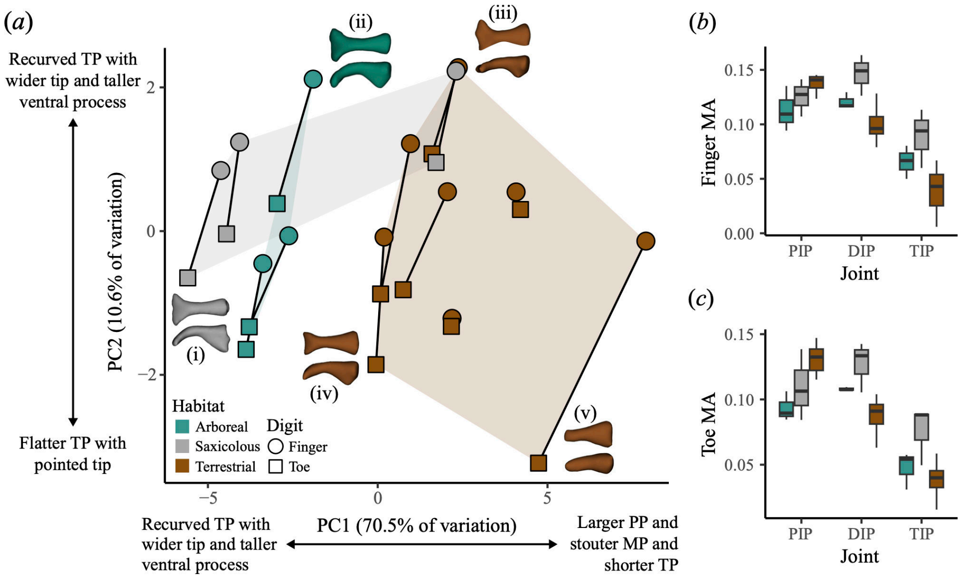

Figure 5. Morphological and functional variation of the phalanges. (*a*) Morphospace of the proximal (PP), penultimate (MP) and terminal (TP) phalanges in the longest finger and toe of each species. Insets depict the dorsal and lateral view of the terminal phalanges in representative species: (i) *A. aeneus*, (ii) *A. lugubris*, (iii) *A. niger*, (iv) *A. iecanus* and (v) *P. elongatus*. (*b*) Mechanical advantage (MA) of the longest finger at the PIP joint, DIP joint and the distal TIP. (*c*) Mechanical advantage of the longest toe at the PIP, DIP and TIP.

that were about 1 µm wide and relatively shallow on their soles but nowhere else (figure 6*e–g*). Large pores, presumed to be mucus pores, were common on the soles (11–25 pores/mm^2) and ventral surface of the toes (8–26 pores/mm^2) but rare on the toe pads of all species (0–2 pores per pad; electronic supplementary material, table S3). One *A. lugubris* specimen had twice the number of large pores on its sole and numerous smaller pores (figure 6*h*) than the other *A. lugubris* specimen. Variation in the epithelial morphology and pore density did not appear to correlate with habitat use.

We categorized the nano-morphologies into four discrete types but note the presence of continuous variation (figure 6*i–l*). Type 1 was composed of numerous spherical structures that appeared unorganized (figure 6*i*) and were found on the toe pads of most species. Type 2 consisted of papillous protrusions that were spaced out (figure 6*j*) and found on the soles of *A. hardii*, *A. lugubris* (but only in the specimen with abundant pores) and *P. elongatus*. In contrast, type 3 had dense clusters of papillae

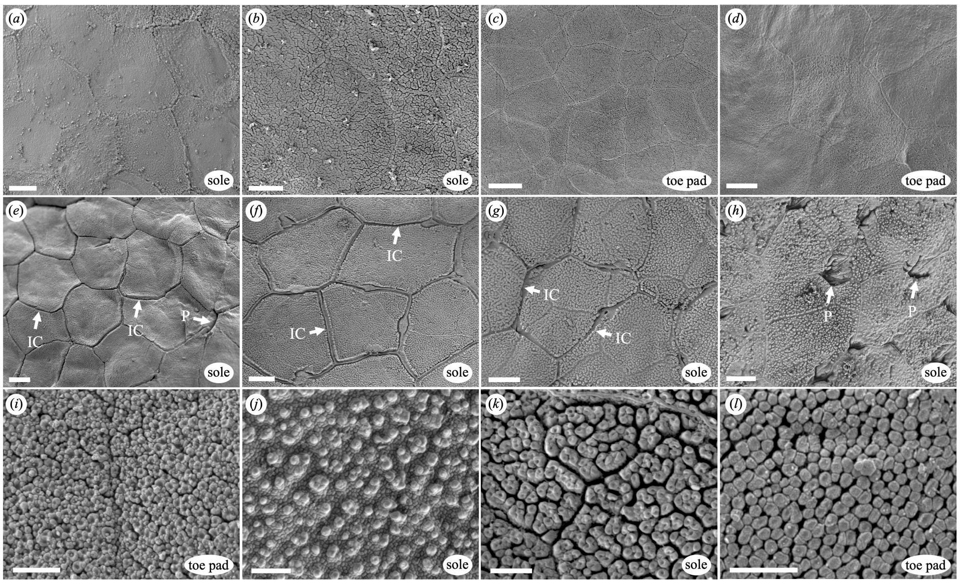

Figure 6. Scanning electron micrographs of the epithelia on the ventral surface of the pes. Smooth sole and toe pad of (*a*) *P. elongatus*, (*b*) *A. vagrans*, (*c*) *P. glutinosus* and (*d*) *A. aeneus* showing the lack of intercellular channels between the polygonal cells. Intercellular channels were observed on the soles of (*e–f*) *A. aeneus* and (*g*) *A. hardii*. (*h*) The sole of an *A. lugubris* specimen with a high density of pores. Nano-morphologies observed in (*i*) *A. niger*, (*j*) *A. lugubris* (same as in (*h*)), (*k*) *A. vagrans* (same as in (*b*)), and (*l*) *P. petraeus*. Abbreviations: IC, intercellular channel; *p*, pore. Scale bar = 10 µm (*a–h*); scale bars = 2 µm (*i–l*).

separated by narrow channels (figure 6*k*) and was found most notably on the soles of *A. vagrans*. Other species—including *A. aeneus*, *A. flavipunctatus*, *A. niger*, the other *A. lugubris* specimen and *P. petraeus*—had sole morphologies that were intermediate between types 2 and 3, in that the papillae varied in size and density. Lastly, type 4 was distinct and consisted of small, densely packed, peg-like structures found on the toes of *P. petraeus* and on the toes and sole of *P. glutinosus* (figure 6*l*). The pegs were loosely polygonal in shape and had central depressions on top (as did the papillae in type 3; electronic supplementary material, figure S3).

4. Discussion

Plethodontid salamanders lack the common morphological adaptations for overcoming gravitational and shear forces observed in other climbing tetrapods [15,16,19]. Instead, we found that scansorial species within *Aneides* and *Plethodon* possess alternate suites of morphological traits that likely augment their clinging, gripping and climbing performance on inclined surfaces. Scansorial species had longer limbs and digits than non-climbers, which is often associated with faster and more stable climbing on broad surfaces [50–52]. Climbers also had disproportionately large autopods and phalangeal morphologies that likely facilitate larger clinging and gripping forces, respectively, compared with non-climbers. Some also had epithelial morphologies that may increase adhesion and friction when clinging. Observations that *A. aeneus* occupy rock crevices further off the ground and cling to steeper angles than other syntopic plethodontids, including *P. glutinosus* support the hypothesis that these traits confer superior climbing abilities [53–55]. However, not all climbers share the characteristics of scansorial *Aneides*, emphasizing the existence of multiple climbing phenotypes [15,17]. Many-to-one mapping may contribute to the abundance of scansorial plethodontids and weak patterns of convergence [16,17] by availing more viable evolutionary pathways towards scansoriality [1,3].

Our findings indicate clear ecomorphological divergence in body shape between the arboreal, saxicolous and terrestrial species examined herein. However, when sampling across Caudata, many climbers do not appear phenotypically distinct from non-climbers [17], suggesting the effects of habitat may be lineage dependent. Nevertheless, the morphologies of arboreal and saxicolous *Aneides* appear fine-tuned for their respective microhabitats. Arboreal species climb on tree bark that is often rugose and with large footholds, whereas saxicolous species commonly climb on sandstone and limestone outcrops that are comparatively smoother (asperity size = 100–200 µm) [20,56]. Frequently climbing on rocks may exert stronger selection for larger autopods and gripping forces because salamander clinging performance decreases on coarse surfaces (asperity size = 100–350 µm) compared with completely smooth (0 µm) and rough surfaces (1000–4000 µm) [15,26]. Indeed, other saxicolous plethodontids also had larger autopods than arboreal species. Saxicolous *Aneides* also had longer tails than arboreal species, but the function of salamander tails is not well-known. Many plethodontids, including *Aneides*, have prehensile tails [57] that could be used like a fifth limb to increase stability and prevent falling [8,58–60], or to grasp the substrate when crossing narrow perches or bridging gaps [57,61]. Additionally, arboreal *Aneides* use their tail in controlled descents after jumping or falling [62]. To better understand the relationship between body shape and habitat, future studies should compare the climbing performance of morphologically and ecologically diverse salamanders on substrates that vary in texture and width.

To maintain consistent clinging performance, morphological traits for attachment should ideally scale proportionally with body mass and the gravitational forces acting to dislodge them (slope = 1) [63]. Although less than one, the static slopes of climbing species of *Aneides* and *Plethodon* exhibited positive allometries that indicate they grow disproportionately large autopods (slope = 0.73–0.92). These findings are unusual because within groups of closely related frogs and lizards, adhesive pads scale closer to isometry (slope = 0.66) and vary more in relative size [63]. Selection can act on static slopes and intercepts, but the latter are often more responsive to selection [63–65]. Static slopes are considered to be constrained by stabilizing selection, so positive allometry is often interpreted as a response to strong directional selection [65,66]. Therefore, selection is likely acting on autopod size in climbing salamanders to increase clinging performance. The positive allometries in terrestrial species of *Aneides* probably represent plesiomorphic conditions and support our finding that the ancestor of *Aneides* was likely scansorial (figure 1).

Moreover, *A. ferreus* and *A. vagrans* exhibited steeper allometries (slope = 0.88−0.92) than the other scansorial species of *Aneides* (slope = 0.73−0.83). *Aneides vagrans* dwell in the canopy of redwood trees as high as 93 m, which is 1.5−5× higher than has been documented for other *Aneides* species [18,21,67,68]. *Aneides vagrans* can also manoeuvre and parachute in the air after jumping to glide down the tree, which is facilitated by their long limbs and large autopods that increase drag [62,69]. *Aneides ferreus* has only been observed 61 m above the ground but, in laboratory settings, they readily jump onto nearby objects, including vertical surfaces [18,67,70]. Environmental challenges imposed by gliding may be aligned with those for climbing, thereby producing a steeper allometric relationship in these species. Alternatively, larger autopods may be attributable to phenotypic plasticity, which could be addressed in future studies that examine the genotype–environment interactions affecting autopod size.

Despite the range of static intercepts and slopes recorded, scansorial plethodontids spanning multiple genera all have relatively larger pes than non-climbing relatives. We propose that scansorial salamanders obtain larger autopods and, thus, superior clinging performance through many-to-one mapping of scaling coefficients [28]. For instance, the arboreal *Bolitoglossa franklini* has isometric pes growth but a higher intercept, which yields relatively large pes and exceptional clinging abilities comparable to those of scansorial *Aneides* [71]. Previously, the pes allometries of *Bolitoglossa* were considered non-adaptive based on the assumption that webbed autopods should exhibit steeper static slopes than unwebbed autopods [29]. In reality, autopod shape is a poor predictor of salamander clinging performance [71], and the webbed autopods of *Bolitoglossa* are the by-product of a shift towards paedomorphic development [29]. Thus, variation in the scaling coefficients enables larger autopod sizes to evolve through selection despite potential constraints on autopod shape. Interestingly, no species examined herein exhibits both a high slope and intercept, potentially reflecting a functional trade-off that limits autopod size.

A few salamander species had pes epithelia that could confer some degree of increased adhesion and friction based on their similarities with frog toe pads [72–74]. The intercellular channels on the soles of the saxicolous *A. aeneus* and terrestrial *A. hardii* were narrower (approximately 1 µm wide) than the channels on the toe pad of the rock frog *Staurios parvus*, but like those found on its subarticular tubercles (0.06−1.6 µm)—secondary adhesive structures on frog toes [73]. Because the channels of *A. aeneus* and *A. hardii* were relatively shallow, they may have a larger role in friction than adhesion [74]. Furthermore, *P. petraeus* and *P. glutinosus* had peg-like nanostructures that resembled those in frogs. The pegs of the two *Plethodon* species were of similar width (approximately 0.33 µm) as the pegs of *S. parvus* (0.2−0.3 µm) and had similar concave depressions at the distal tips of the pegs [72,73] (electronic supplementary material, figure S3). These similarities suggest that the *Plethodon* nanopillars may aid in adhesion or friction. However, thick mucus layers on the pedes could reduce the effectiveness of salamander nanostructures (channels or pillars) by preventing interactions with the surface [75]. That said, all species examined herein as well as terrestrial *Bolitoglossa* have relatively low densities of putative mucus pores across their pedes (8–26 and 13–21 pores/mm^2, respectively) compared with arboreal *Bolitoglossa* (47–68 pores/mm^2) and a frog (*Hyla cinerea*) toe pad (53 pores/mm^2) [76,77]. That suggests scansorial *Bolitoglossa* and at least some scansorial frogs utilize mucus adhesion more than scansorial *Aneides* or *Plethodon*.

The inconsistent distribution of presumably advantageous epithelial morphologies among scansorial salamanders raises doubt about whether they are adaptive. Intercellular channels are also absent in terrestrial and arboreal *Bolitoglossa* but present in some semi-aquatic *Desmognathus* salamanders that also have keratinous toe tips, possibly for station holding in streams [76,78]. Seeing how torrent frogs also have intercellular channels that they use to drain excess fluid from under their pads [79], wet environments may promote the evolution of channels, but *A. niger*, which exhibits some semi-aquatic tendencies [80], lacks channels. Meanwhile, *A. vagrans*, and likely other species of *Aneides*, can potentially modulate the compliance of their toe pads and adhesion through fine control over the perfusion of blood into their digits [24]. Draining their digits would enable the distal tips to deform around small surface asperities and increase friction [81,82]. Indeed, it was observed that the toe epithelium of *A. vagrans* folded and formed large pleats when the animal was dragged across a surface [24]. These observations suggest the material properties of autopod epithelium may be more important for climbing than its microstructures.

Some salamanders can compensate for lower clinging performance on rough surfaces by gripping surface asperities with their digits [19,26]. We found that scansorial species of *Aneides* and *Plethodon* have larger ventral processes on their terminal phalanges than terrestrial species. That changes the insertion angle of the flexor tendon, increases force production, and mitigates the functional trade-off between gripping force and digit length. Climbers also had shorter proximal phalanges and slightly longer distal ones, another strategy for enhancing gripping force without sacrificing reach [32]. Furthermore, climbers had more recurved terminal phalanges that were laterally expanded at the distal tip, which may decrease bone strain when grasping and increase the stiffness of the digit [24,33]. Other salamanders also have expanded terminal phalanges but it appears unrelated to habitat preferences [83]. Instead, locomotor mode (climbing versus non-climbing) may be a better predictor of phalangeal morphology. *Plethodon cinereus* has phalanges resembling those of *P. elongatus* (flat and pointed) [84], which might explain its inability to climb on coarse vertical surfaces [15]. Climbing frogs also have expanded phalanges, providing additional evidence for their broad adaptive significance [85]. A more comprehensive comparison of phalangeal morphology might reveal that climbing salamanders have repeatedly evolved phenotypes that support gripping.

5. Conclusions

Integrating data across multiple levels of biological organization, from whole organisms to cells, helped us identify potential morphological adaptations that assist some scansorial salamanders. Because many-to-one mapping is prevalent across Plethodontidae, it is unclear to what extent our findings describe the ecomorphological patterns of scansorial lineages across the family. There are other scansorial lineages (*Eurycea* spp. and *Nyctanolis pernix*) with long limbs and large autopods that seem to resemble *Aneides* and *Plethodon*. However, many genera (i.e. *Bolitoglossa*, *Chiropterotriton* and *Speleomantes*) have webbed autopods and truncated digits [28,29] that contrast the dexterous digits in scansorial species of *Aneides*. The different suites of climbing morphologies likely reflect multiple factors, including separate evolutionary origins of scansoriality, different developmental pathways or preferences for microhabitats with different structural properties (i.e. width, texture and compliance). Yet, scansorial species of *Aneides* and *Bolitoglossa* have relatively large pedes and expanded terminal phalanges [28], suggesting that some traits are convergent across a broader phylogenetic scale than others. We propose that the traits studied herein represent axes of variation by which salamanders can vary their arsenal of climbing morphologies. Future studies should assess the role of constraints and environmental demands in structuring patterns of morphological convergence across climbing salamanders.

Ethics. This work did not require ethical approval from a human subject or animal welfare committee.

Data accessibility. The morphological data and script files used for this study can be found on Dryad [86]. All CT scans have been uploaded to MorphoSource (see electronic supplemental material).

Supplementary material is available online [87].

Declaration of AI use. We have not used AI-assisted technologies in creating this article.

Authors' contributions. J.M.H.: conceptualization, data curation, formal analysis, funding acquisition, investigation, methodology, visualization, writing—original draft; G.P.: data curation, investigation, writing—review and editing; S.K.: conceptualization, funding acquisition, methodology, resources, supervision, writing—review and editing.

All authors gave final approval for publication and agreed to be held accountable for the work performed therein.

Conflict of interests. We declare we have no competing interests.

Funding. This work was supported by a US National Science Foundation Graduate Research Fellowship (DGE-1746914), a Washington Biology Field Club Award and American Society for Ichthyology and Herpetology Gaige Fund Award to J.M.H.; as well as an American Association of University Women Research Publication Grant (015943) to S.M.K.

Acknowledgements. We thank the museum and collections staff who facilitated access to specimens, including A. Wynn and E. Langan (NMNH), C. Spencer (MVZ), L. Scheinberg (CAS) and J. Beane and B. Stuart (NCSM), as well as G. Schneider and A. Jones (UMMZ) for photographing and measuring an *A. caryaensis* specimen. We also appreciate T. Hsu (NMNH) for micro-CT scanning specimens, N. Staub for helpful conversations and data, D. Adams for providing data and code and P. Tardelli for their help with scanning electron microscopy. Lastly, we thank two anonymous reviewers for their helpful comments. Portions of this work were developed from the doctoral thesis of J.M.H.

References

1. Wainwright PC, Alfaro ME, Bolnick DI, Hulsey CD. 2005 Many-to-one mapping of form to function: a general principle in organismal design? *Integr. Comp. Biol*. **45**, 256–262. (doi:10.1093/icb/45.2.256)
2. Kolmann MA, Huie JM, Evans K, Summers AP. 2018 Specialized specialists and the narrow niche fallacy: a tale of scale-feeding fishes. *R. Soc. Open Sci*. **5**, 171581. (doi:10.1098/rsos.171581)
3. Moen DS. 2019 What determines the distinct morphology of species with a particular ecology? The roles of many-to-one mapping and trade-offs in the evolution of frog ecomorphology and performance. *Am. Nat*. **194**, E81–E95. (doi:10.1086/704736)
4. Sustaita D, Pouydebat E, Manzano A, Abdala V, Hertel F, Herrel A. 2013 Getting a grip on tetrapod grasping: form, function, and evolution. *Biol. Rev*. **88**, 380–405. (doi:10.1111/brv.12010)
5. Cartmill M. 1974 Pads and claws in arboreal locomotion. *Primate Locomot*. **1**, 43–83.
6. Preuschoft H. 2002 What does 'arboreal locomotion' mean exactly and what are the relationships between 'climbing, environment and morphology? *Z. Für Morphol. Anthropol.* **83**, 171–188. (doi:10.1127/zma/83/2002/171)
7. Young MW, Flaim ND, Virga JQ, Kantounis SK, Granatosky MC. 2024 Mechanical constraints during vertical climbing reveals limited deviation from theoretical minima. *Integr. Comp. Biol*. **64**, 145–155. (doi:10.1093/icb/icae029)
8. Young MW *et al*. 2024 What does climbing mean exactly? Assessing spatiotemporal gait characteristics of inclined locomotion in parrots. *J. Comp. Physiol. A* **210**, 19–33. (doi:10.1007/s00359-023-01630-0)
9. Crandell KE, Herrel A, Sasa M, Losos JB, Autumn K. 2014 Stick or grip? Co-evolution of adhesive toepads and claws in *Anolis* lizards. *Zoology* **117**, 363–369. (doi:10.1016/j.zool.2014.05.001)
10. Wolff JO, Gorb SN. 2016 Mechanical attachment devices. In *Attachment structures and adhesive secretions in arachnids* (eds JO Wolff, SN Gorb), pp. 25–52. Cham, Switzerland: Springer International Publishing. (doi:10.1007/978-3-319-45713-0_2)
11. Huie JM, Prates I, Bell RC, de Queiroz K. 2021 Convergent patterns of adaptive radiation between island and mainland *Anolis* lizards. *Biol. J. Linn. Soc*. **134**, 85–110. (doi:10.1093/biolinnean/blab072)
12. Miller AH, Stroud JT. 2021 Novel tests of the key innovation hypothesis: adhesive toepads in arboreal lizards. *Syst. Biol*. **71**, 139–152. (doi:10.1093/sysbio/syab041)
13. Zimin A, Zimin SV, Grismer LL, Bauer AM, Chapple DG, Dembitzer J, Roll U, Meiri S. 2024 Microhabitat and adhesive toepads shape gecko limb morphology. *Integr. Zool*. **20**, 634–650. (doi:10.1111/1749-4877.12880)
14. Basham EW, González-Pinzón M, Romero-Marcucci A, Carl N, Baecher JA, Scheffers BR. 2022 Large, old trees define the vertical, horizontal, and seasonal distributions of a poison frog. *Oecologia* **199**, 257–269. (doi:10.1007/s00442-022-05108-9)

15. Hanna CS, Alihosseini C, Fischer HM, Davoli EC, Granatosky MC. 2022 Are they arboreal? Climbing abilities and mechanics in the red-backed salamander (*Plethodon cinereu*). *J. Exp. Zool. A Ecol. Integr. Physiol.* **337**, 238–249. (doi:10.1002/jez.2561)
16. McEntire KD. 2016 Arboreal ecology of plethodontidae: a review. *Copeia* **104**, 124–131. (doi:10.1643/ot-14-214)
17. Baken EK, Adams DC. 2019 Macroevolution of arboreality in salamanders. *Ecol. Evol*. **9**, 7005–7016. (doi:10.1002/ece3.5267)
18. Spickler J, Sillett S, Marks S, Welsh H. 2006 Evidence of a new niche for a North American salamander: *Aneides vagrans* residing in the canopy of old-growth redwood forest. *Herpetol. Conserv. Biol*. **1**.
19. Aretz JM, Brown CE, Deban SM. 2022 Vertical locomotion in the arboreal salamander *Aneides vagrans*. *J. Zool*. **316**, 72–79. (doi:10.1111/jzo.12934)
20. Gordon RE. 1952 A contribution to the life history and ecology of the Plethodontid Salamander *Aneides aeneus* (Cope and Packard). *Am. Midl. Nat.* **47**, 666–701. (doi:10.2307/2422035)
21. Waldron JL, Humphries WJ. 2005 Arboreal habitat use by the *Green salamander*, *Aneides aeneus*, in South Carolina. *J. Herpetol.* **39**, 486–492. (doi:10.1670/228-04A.1)
22. Wake DB. 1963 Comparative osteology of the plethodontid salamander genus *Aneides*. *J. Morphol*. **113**, 77–118. (doi:10.1002/jmor.1051130106)
23. Larson A, Wake DB, Maxson LR, Highton R. 1981 A molecular phylogenetic perspective on the origins of morphological novelties in the salamanders of the Tribe Plethodontini (Amphibia, plethodontidae). *Evolution* **35**, 405–422. (doi:10.1111/j.1558-5646.1981.tb04902.x)
24. Brown CE, Goldenberg WP, Hinds OM, O'Donnell MK, Staub NL. 2025 Vascular and osteological morphology of expanded digit tips suggests specialization in the wandering salamander (*Aneides vagrans*). *J. Morphol*. **286**, e70026. (doi:10.1002/jmor.70026)
25. Riedel J, Vucko MJ, Blomberg SP, Robson SKA, Schwarzkopf L. 2019 Ecological associations among epidermal microstructure and scale characteristics of Australian geckos (Squamata: Carphodactylidae and Diplodactylidae). *J. Anat*. **234**, 853–874. (doi:10.1111/joa.12969)
26. O'Donnell MK, Deban SM. 2020 The effects of roughness and wetness on salamander cling performance. *Integr. Comp. Biol*. **60**, 840–851. (doi:10.1093/icb/icaa110)
27. O'Donnell MK, Deban SM. 2020 Cling performance and surface area of attachment in plethodontid salamanders. *J. Exp. Biol*. **223**, b211706. (doi:10.1242/jeb.211706)
28. Alberch P. 1981 Convergence and parallelism in foot morphology in the neotropical salamander genus *Bolitoglossa*. I. Function. *Evolution* **35**, 84–100. (doi:10.1111/j.1558-5646.1981.tb04861.x)
29. Jaekel M, Wake DB. 2007 Developmental processes underlying the evolution of a derived foot morphology in salamanders. *Proc. Natl Acad. Sci. USA* **104**, 20437–20442. (doi:10.1073/pnas.0710216105)
30. Adams DC, Nistri A. 2010 Ontogenetic convergence and evolution of foot morphology in European cave salamanders (Family: Plethodontidae). *BMC Evol. Biol*. **10**, 216. (doi:10.1186/1471-2148-10-216)
31. Langowski JKA, Dodou D, Kamperman M, van Leeuwen JL. 2018 Tree frog attachment: mechanisms, challenges, and perspectives. *Front. Zool*. **15**, 32. (doi:10.1186/s12983-018-0273-x)
32. Dickinson E, Young MW, Flaim ND, Sawiec A, Granatosky MC. 2023 A functional framework for interpreting phalangeal form. *J. R. Soc. Interface* **20**, 20230251. (doi:10.1098/rsif.2023.0251)
33. Richmond BG. 2007 Biomechanics of phalangeal curvature. *J. Hum. Evol*. **53**, 678–690. (doi:10.1016/j.jhevol.2007.05.011)
34. Wynn AH, Highton R, Jacobs JF. 1988 A new species of rock-crevice dwelling *Plethodon* from Pigeon Mountain, Georgia. *Herpetologica* **44**, 135–143.
35. Jensen JB, Camp CD, Marshall JL. 2002 Ecology and life history of the Pigeon Mountain salamander. *Southeast. Nat*. **1**, 3–16. (doi:10.1656/1528-7092(2002)001)
36. Stewart AA, Wiens JJ. 2024 A time-calibrated salamander phylogeny including 765 species and 503 genes. *Mol. Phylogenet. Evol.* **204**, 108272. (doi:10.1016/j.ympev.2024.108272)
37. Revell LJ. 2024 Phytools 2.0: an updated R ecosystem for phylogenetic comparative methods (and other things). *PeerJ* **12**, e16505. (doi:10.7717/peerj.16505)
38. R Core Team. 2023 R: A Language and Environment for Statistical Computing. Vienna, Austria: R Foundation for Statistical Computing. See https://www.R-project.org/.
39. Adams DC, Korneisel D, Young M, Nistri A. 2017 Natural history constrains the macroevolution of foot morphology in European Plethodontid salamanders. *Am. Nat*. **190**, 292–297. (doi:10.1086/692471)
40. Bingham RE, Papenfuss TJ, Lindstrand L, Wake DB. 2018 Phylogeography and species boundaries in the *Hydromantes shastae* complex, with description of two new species (Amphibia; Caudata; Plethodontidae). *Bull. Mus. Comp. Zool.* **161**, 403–427. (doi:10.3099/MCZ42.1)
41. Schindelin J *et al*. 2012 Fiji: an open-source platform for biological-image analysis. *Nat. Methods* **9**, 676–682. (doi:10.1038/nmeth.2019)
42. Warton DI, Duursma RA, Falster DS, Taskinen S. 2012 smatr 3– an R package for estimation and inference about allometric lines. *Methods Ecol. Evol*. **3**, 257–259. (doi:10.1111/j.2041-210x.2011.00153.x)
43. Baken EK, Collyer ML, Kaliontzopoulou A, Adams DC. 2021 Geomorph v4.0 and gmShiny: enhanced analytics and a new graphical interface for a comprehensive morphometric experience. *Methods Ecol. Evol*. **12**, 2355–2363. (doi:10.1111/2041-210x.13723)
44. Santini L, Benítez-lópez A, Ficetola GF, Huijbregts MAJ. 2018 Length–mass allometries in amphibians. *Integr. Zool*. **13**, 36–45. (doi:10.1111/1749-4877.12268)
45. Boyer DM, Gunnell GF, Kaufman S, McGeary TM. 2016 MorphoSource: archiving and sharing 3-D digital specimen. *Paleontol. Soc. Pap.* **22**, 157–181. (doi:10.1017/scs.2017.13)
46. Blackburn DC *et al*. 2024 Increasing the impact of vertebrate scientific collections through 3D imaging: the openVertebrate (oVert) thematic collections network. *BioScience* **74**, 169–186. (doi:10.1093/biosci/biad120)
47. Kikinis R, Pieper SD, Vosburgh KG. 2014 3D Slicer: a platform for subject-specific image analysis, visualization, and clinical support. In *Intraoperative imaging and image-guided therapy* (ed. FA Jolesz), pp. 277–289. New York, NY: Springer. (doi:10.1007/978-1-4614-7657-3_19)
48. Rolfe S *et al*. 2021 SlicerMorph: an open and extensible platform to retrieve, visualize and analyse 3D morphology. *Methods Ecol. Evol*. **12**, 1816–1825. (doi:10.1111/2041-210x.13669)
49. Zani. 2000 The comparative evolution of lizard claw and toe morphology and clinging performance. *J. Evol. Biol.* **13**, 316–325. (doi:10.1046/j.1420-9101.2000.00166.x)
50. Losos JB, Sinervo B. 1989 The effects of morphology and perch diameter on sprint performance of *Anolis* lizards. *J. Exp. Biol*. **145**, 23–30. (doi:10.1242/jeb.145.1.23)
51. Lammers AR, Zurcher U. 2011 Stability during arboreal locomotion. In *Theoretical biomechanics*, pp. 319–334. London: IntechOpenCity. (doi:10.5772/23751)
52. Granatosky MC, McElroy EJ, Laird MF, Iriarte-Diaz J, Reilly SM, Taylor AB, Ross CF. 2019 Joint angular excursions during cyclical behaviors differ between tetrapod feeding and locomotor systems. *J. Exp. Biol*. **222**, jeb200451. (doi:10.1242/jeb.200451)
53. Cliburn J, Porter A. 1986 Comparative climbing abilities of the salamanders *Aneides aeneus* and *Plethodon glutinosus* (Caudata, Plethodontidae). *J. Miss. Acad. Sci. Miss. Acad. Sci*. **31**, 91–96.
54. Cliburn J, Porter A. 1987 Vertical stratification of the salamanders *Aneides aeneus* and *Plethodon glutinosus* (Caudata, Plethodontidae). *J. Ala. Acad. Sci*. **58**, 18–22.
55. Waldron JL. 2000 *Ecology and sympatric relations of crevice salamanders in randolph county*. West Virginia, USA: Marshall University. See https://mds.marshall.edu/etd/1705/.
56. Kitty LM. 2001 Diagenetic heterogeneity in sandstone at the outcrop scale, Breathitt Formation (Pennsylvanian), eastern Kentucky. *AAPG Bull* **85**, 795–815. (doi:10.1306/8626CA05-173B-11D7-8645000102C1865D)

57. Dickie R. 1999 Structure-function relationships in the evolutionary morphology of the plethodontid tail. PhD, [Berkeley, CA, USA]: University of California. https://www.proquest.com/docview/304495854/abstract/EA54DCA6833842F9PQ/1.
58. Stebbins RC. 1947 Tail and foot action in the locomotion of hydromantes platycephalus. *Copeia* **1947**, 1–5. (doi:10.2307/1438886)
59. Jusufi A, Goldman DI, Revzen S, Full RJ. 2008 Active tails enhance arboreal acrobatics in geckos. *Proc. Natl Acad. Sci. USA* **105**, 4215–4219. (doi:10.1073/pnas.0711944105)
60. Dickinson E, Young MW, DeLeon D, Bas B, Zou B, Ratkiewicz A, Beatty BL, Granatosky MC. 2023 Tail feather strength in tail-assisted climbing birds is achieved through geometric, not material change. *Proc. R. Soc. B* **290**, 20222325. (doi:10.1098/rspb.2022.2325)
61. Luger A, Vermeylen V, Herrel A, Adriaens D. 2021 Do substrate roughness and gap distance impact gap-bridging strategies in arboreal chameleons? *Belg. J. Zool* **151**, 31–45. (doi:10.26496/bjz.2021.83)
62. Brown CE, Sathe EA, Dudley R, Deban SM. 2022 Aerial maneuvering by plethodontid salamanders spanning an arboreality gradient. *J. Exp. Biol*. **225**, jeb244598. (doi:10.1242/jeb.244598)
63. Labonte D, Clemente CJ, Dittrich A, Kuo CY, Crosby AJ, Irschick DJ, Federle W. 2016 Extreme positive allometry of animal adhesive pads and the size limits of adhesion-based climbing. *Proc. Natl Acad. Sci. USA* **113**, 1297–1302. (doi:10.1073/pnas.1519459113)
64. Egset CK, Hansen TF, Le rouzic A, Bolstad GH, Rosenqvist G, Pélabon C. 2012 Artificial selection on allometry: change in elevation but not slope. *J. Evol. Biol*. **25**, 938–948. (doi:10.1111/j.1420-9101.2012.02487.x)
65. Pélabon C, Firmat C, Bolstad GH, Voje KL, Houle D, Cassara J, Rouzic AL, Hansen TF. 2014 Evolution of morphological allometry. *Ann. N. Y. Acad. Sci*. **1320**, 58–75. (doi:10.1111/nyas.12470)
66. Bonduriansky R, Day T. 2003 The evolution of static allometry in sexually selected traits. *Evolution* **57**, 2450–2458. (doi:10.1111/j.0014-3820.2003.tb01490.x)
67. Jones LL, Leonard WP, Olson DH. 2005 *Amphibians of the pacific northwest*. Seattle, WA: Seattle Audubon Society.
68. Forsman ED, Swingle JK. 2007 Use of arboreal nests of tree voles (*Arborimus* spp.) by amphibians. *Herpetol. Conserv. Biol*. **2**, 113–118.
69. Brown CE, Kirk AM. 2023 Characterizing lift, drag, and pressure differences across wandering salamanders (*Aneides vagrans*) with computational fluid dynamics to investigate aerodynamics. *J. Morphol*. **284**, e21583. (doi:10.1002/jmor.21583)
70. Nussbaum RA, Brodie ED, Storm RM. 1983 *Amphibians and reptiles of the Pacific northwest*. Moscow, Idaho: University Press of Idaho.
71. Baken EK, O'Donnell MK. 2021 Clinging ability is related to particular aspects of foot morphology in salamanders. *Ecol. Evol*. **11**, 11000–11008. (doi:10.1002/ece3.7888)
72. Barnes WJP, Baum M, Peisker H, Gorb SN. 2013 Comparative Cryo-SEM and AFM studies of hylid and rhacophorid tree frog toe pads. *J. Morphol*. **274**, 1384–1396. (doi:10.1002/jmor.20186)
73. Drotlef DM, Appel E, Peisker H, Dening K, del Campo A, Gorb SN, Barnes WJonP. 2015 Morphological studies of the toe pads of the rock frog, *Staurois parvus* (family: Ranidae) and their relevance to the development of new biomimetically inspired reversible adhesives. *Interface Focus* **5**, 20140036. (doi:10.1098/rsfs.2014.0036)
74. Endlein T, Ji A, Yuan S, Hill I, Wang H, Barnes WJP, Dai Z, Sitti M. 2017 The use of clamping grips and friction pads by tree frogs for climbing curved surfaces. *Proc. R. Soc. B* **284**, 20162867. (doi:10.1098/rspb.2016.2867)
75. Wainwright DK, Lauder GV. 2017 Mucus matters: the slippery and complex surfaces of fish. In *Functional surfaces in biology III: diversity of the physical phenomena* (eds SN Gorb, EV Gorb), pp. 223–246. Cham, Switzerland: Springer International Publishing. (doi:10.1007/978-3-319-74144-4_10)
76. Green DM, Alberch P. 1981 Interdigital webbing and skin morphology in the neotropical salamander genus *Bolitoglossa* (Amphibia; Plethodontidae). *J. Morphol.* **170**, 273–282. (doi:10.1002/jmor.1051700302)
77. Langowski JKA *et al*. 2019 Comparative and functional analysis of the digital mucus glands and secretions of tree frogs. *Front. Zool*. **16**, 19. (doi:10.1186/s12983-019-0315-z)
78. Caldwell RS, Trauth SE. 1979 Use of the toe pad and tooth morphology in differentiating three species of *Desmognathus* (Amphibia, Urodela). *J. Herpetol.* **13**, 491. (doi:10.2307/1563486)
79. Endlein T, Barnes WJP, Samuel DS, Crawford NA, Biaw AB, Grafe U. 2013 Sticking under wet conditions: the remarkable attachment abilities of the torrent frog, *Staurois guttatus*. *PLoS One* **8**, e73810. (doi:10.1371/journal.pone.0073810)
80. Reilly SB, Wake DB. 2019 Taxonomic revision of black salamanders of the *Aneides flavipunctatus* complex (Caudata: Plethodontidae). *PeerJ* **7**, e7370. (doi:10.7717/peerj.7370)
81. Langowski JKA, Schipper H, Blij A, van den Berg FT, Gussekloo SWS, van Leeuwen JL. 2018 Force-transmitting structures in the digital pads of the tree frog *Hyla cinerea* : a functional interpretation. *J. Anat*. **233**, 478–495. (doi:10.1111/joa.12860)
82. Huie JM, Summers AP. 2022 The effects of soft and rough substrates on suction-based adhesion. *J. Exp. Biol* **225**, jeb243773. (doi:10.1242/jeb.243773)
83. Ponssa ML, Fratani J, Barrionuevo JS. 2022 Phalanx morphology in salamanders: a reflection of microhabitat use, life cycle or evolutionary constraints? *Zoology* **154**, 126040. (doi:10.1016/j.zool.2022.126040)
84. Hanken J, Dinsmore CE. 1986 Geographic variation in the limb skeleton of the red-backed salamander, *Plethodon cinereus*. *J. Herpetol.* **20**, 97–101. (doi:10.2307/1564136)
85. Kamermans M, Vences M. 2009 Terminal phalanges in ranoid frogs: morphological diversity and evolutionary correlation with climbing habits. *Alytes* **26**, 117–152.
86. Huie JM, Park G, Kawano SM. 2025 Salamander ecomorphology reveals a unique suite of climbing adaptations [Dataset]. Dryad Digital Repository. (doi:10.5061/dryad.n02v6wx96)
87. Huie JM, Park G, Kawano S. 2025 Supplementary material from: Salamander ecomorphology reveals a unique suite of climbing adaptations. Figshare. (doi:10.6084/m9.figshare.c.7963826)